neurocritical care society Neurocrit Care (2014) 20:193–201
DOI 10.1007/s12028-013-9917-z

ORIGINAL ARTICLE

Glyburide is Associated with Attenuated Vasogenic Edema in Stroke Patients

W. Taylor Kimberly · Thomas W. K. Battey · Ly Pham · Ona Wu · Albert J. Yoo · Karen L. Furie · Aneesh B. Singhal · Jordan J. Elm · Barney J. Stern · Kevin N. Sheth

Published online: 26 September 2013

Abstract
Background Brain edema is a serious complication of ischemic stroke that can lead to secondary neurological deterioration and death. Glyburide is reported to prevent brain swelling in preclinical rodent models of ischemic stroke through inhibition of a non-selective channel composed of sulfonylurea receptor 1 and transient receptor potential cation channel subfamily M member 4. However, the relevance of this pathway to the development of cerebral edema in stroke patients is not known.
Methods Using a case–control design, we retrospectively assessed neuroimaging and blood markers of cytotoxic and vasogenic edema in subjects who were enrolled in the glyburide advantage in malignant edema and stroke-pilot (GAMES-Pilot) trial. We compared serial brain magnetic resonance images (MRIs) to a cohort with similar large volume infarctions. We also compared matrix metalloproteinase-9 (MMP-9) plasma level in large hemispheric stroke.
Results We report that IV glyburide was associated with T2 fluid-attenuated inversion recovery signal intensity ratio on brain MRI, diminished the lesional water diffusivity between days 1 and 2 (pseudo-normalization), and reduced blood MMP-9 level.
Conclusions Several surrogate markers of vasogenic edema appear to be reduced in the setting of IV glyburide treatment in human stroke. Verification of these potential imaging and blood biomarkers is warranted in the context of a randomized, placebo-controlled trial.

Electronic supplementary material The online version of this article (doi:10.1007/s12028-013-9917-z) contains supplementary material, which is available to authorized users.

W. T. Kimberly · T. W. K. Battey · L. Pham
Center for Human Genetic Research and Division of Neurocritical Care and Emergency Neurology, Massachusetts General Hospital, Harvard Medical School, Boston, MA, USA

W. T. Kimberly · O. Wu
Athinoulo A. Martinos Center for Biomedical Imaging, Massachusetts General Hospital, Harvard Medical School, Boston, MA, USA

W. T. Kimberly · A. B. Singhal
Stroke Service, Massachusetts General Hospital, Harvard Medical School, Boston, MA, USA

W. T. Kimberly (✉)
Lunder 644, 55 Fruit St, Boston, MA 02114, USA
e-mail: wtkimberly@partners.org

A. J. Yoo
Division of Neuroradiology, Massachusetts General Hospital, Harvard Medical School, Boston, MA, USA

K. L. Furie
Department of Neurology, Warren Alpert Medical School of Brown University, Providence, RI, USA

J. J. Elm
Division of Biostatistics and Epidemiology, Medical University of South Carolina, Charleston, NC, USA

B. J. Stern
Department of Neurology and Emergency Medicine, University of Maryland School of Medicine, Baltimore, MD, USA

K. N. Sheth
Division of Neurocritical Care and Emergency Neurology, Department of Neurology, Yale Medical School and Yale New Haven Hospital, New Haven, CT, USA

Keywords Stroke · Cerebral edema · Glyburide · Biomarker

Introduction

Brain edema is a common secondary complication after large hemispheric stroke [1, 2]. Following the initial ischemic event, swelling can lead to worsening of neurological function that often manifests within the first 2 days [3]. Edema can be particularly devastating with large hemispheric infarction, resulting in brain herniation and death [4]. Currently, decompressive craniectomy is the only therapy that may improve outcome [5, 6]. However, it is not suitable for all patients [7] and although the procedure reduces mortality, it may also increase the number of severely impaired individuals.

Brain edema can be categorized into cytotoxic and vasogenic types [8], each associated with specific features on brain magnetic resonance imaging (MRI). Apparent diffusion coefficient (ADC) maps are sensitive to cytotoxic edema in the early stages of infarction [9], as water diffusion becomes restricted due to its shift from extracellular to intracellular compartments [2]. The severity of the initial cytotoxic ischemia can influence subsequent brain swelling [10–12], which is dependent upon blood flow and, therefore, termed vasogenic edema [2, 8]. Two MRI sequences are sensitive to vasogenic edema, including T2 fluid-attenuated inversion recovery (FLAIR) [13] and ADC pseudo-normalization [14]. In addition, circulating matrix metalloproteinase-9 (MMP-9) level is associated with blood–brain barrier (BBB) breakdown after stroke [15]. Excessive MMP-9 activity can contribute to vasogenic edema [16], and, if BBB integrity is sufficiently impaired, can further lead to hemorrhagic transformation [17].

Preclinical data implicate a non-selective calcium-activated channel in the development of ischemic brain swelling [18]. A non-selective composed of sulfonylurea receptor 1 (SUR1) and transient receptor potential cation channel subfamily M member 4 (TRPM4); inhibition of this channel reduced brain swelling and mortality in rodent models of stroke [19]. In vitro and in vivo evidence supports a role for the channel in mediating cytotoxic edema [20] and vasogenic edema [19, 21]. However, the extent to which the channel has a role in human stroke patients is unknown. We retrospectively analyzed subjects from the glyburide advantage in malignant edema and stroke-pilot (GAMES-Pilot) and compared them to separate cohorts with large infarction in order to evaluate potential imaging and blood biomarkers of edema.

Materials and Methods

Patients

Eligible patients were between the ages of 18 and 80 years and presented with a large anterior acute ischemic stroke. The study drug was started within 10 h of the last seen well time, and heparinized plasma samples were collected at baseline and 8 time points during the 72-h drug infusion. Serial brain MRIs were obtained at baseline prior to study drug infusion and at approximately 24, 48, and 72 h after the study drug initiation using a standardized protocol.

The control cohorts were derived from subjects enrolled in either of two protocols at a single institution, as part of the specialized programs of translational research in acute stroke (SPOTRIAS) network. The neuroimaging control cohort included placebo-treated subjects from the normobaric oxygen therapy in acute ischemic stroke trial (NBO). Subjects were eligible for this study if they were $\geq$18 years old and had an acute stroke confirmed by neuroimaging. As part of the study plan, serial brain MRIs were obtained at baseline and at approximately 6, 24, and 48 h after enrollment. From the total of 49 placebo-treated subjects, those selected for comparison with GAMES-Pilot had DWI infarct volume $>$55 cc ($N = 8$). We selected this volume cut-off based on the planimetric baseline DWI volumes of the GAMES-Pilot cohort, which were all $>$54 cc. The control cohort for MMP-9 levels was derived from a prospectively collected biomarker repository. Subjects were eligible if they were $\geq$18 years old and had an acute stroke that presented within 9 h from stroke onset. Biomarker control subjects were selected for comparison with the GAMES-Pilot cohort if they had available plasma samples at approximately 48 h and had a baseline stroke volume $>$55 cc ($N = 15$).

All subjects or their legally authorized representatives provided written informed consent, and this study was approved by the local institutional review boards.

MRI Acquisition and Imaging Data Processing

All neuroimaging subjects underwent baseline MRI as part of their acute stroke evaluation. Brain MRI included DWI, ADC, T2 fluid-attenuated inversion recovery (FLAIR), and gradient echo sequences. A standardized imaging acquisition protocol was used. All scans were de-identified and randomized with an ID code. All analyses were conducted blinded to patient and treatment identity. MRI data in raw DICOM format were converted to Neuroimaging Informatics Technology Initiative (NIfTI) format using MRIConvert (Lewis Center for Neuroimaging, University of Oregon,

Eugene, OR). Image files were then loaded into Analyze 11.0 (AnalyzeDirect, Overland Park, KS, USA) for co-registration, manipulation, and quantitative analysis.

Imaging Analysis

Region of interest (ROI) analysis by two independent readers (T.W.K.B and A.J.Y.) was used to generate DWI lesion volumes using Analyze 11.0 (AnalyzeDirect, Overland Park, KS, USA). Pearson correlation was 0.97 ($p < 0.001$) with an intraclass correlation coefficient of 0.98. Bland–Altman plots were examined to verify that there was no systematic bias between raters (see Supplemental Fig. 1).

Signal intensity ratios were calculated by normalizing the signal intensity within the stroke ROI to the signal intensity of the contralateral hemisphere (see Supplemental Fig. 2). The region of stroke and contralateral hemisphere were first defined on DWI. This ROI was subsequently applied to the ADC map to exclude CSF spaces greater than approximately 2 mm for the final stroke ROI and volume measurements. ADC ratios were obtained by normalizing the ADC value within the stroke ROI to the contralateral hemisphere. Signal intensity ratios were calculated by normalizing the signal intensity within the stroke ROI to the signal intensity of the contralateral hemisphere.

FLAIR sequences were co-registered to the ADC map, and the stroke and contralateral hemisphere ROIs were applied to the co-registered FLAIR sequence with visual inspection to confirm proper alignment. FLAIR signal intensity ratios were generated from the stroke FLAIR value normalized to the contralateral hemisphere. Segmentation of the white matter (WM) and gray matter (GM) was performed by applying threshold segmentation to a co-registered fractional anisotropy (FA) map. Threshold segmentation was first conducted to remove GM from the existing stroke and contralateral hemisphere ROIs, followed by re-application of the initial ROI and inversion of the threshold values to subtract WM. These segmented ROIs were then applied to the co-registered FLAIR sequence to generate GM and WM signal intensity ratios.

MMP-9 Analysis

Peripheral blood samples were collected in EDTA-containing or lithium heparin-containing tubes and plasma was immediately separated from cellular material by centrifugation ($1{,}000 \times g$ for 15 min). All samples were centrifuged and separated from the cellular pellet within 60 min of collection. A subset of GAMES-Pilot subjects had both EDTA and heparinized plasma available at the same time points, and MMP-9 values were equivalent between EDTA and heparinized plasma (see Supplemental Fig. 3a). Two out of 55 total GAMES-Pilot blood samples were grossly hemolyzed and were not included in the analysis (see Supplemental Fig. 3b). Supernatant was aliquoted into cryo-vials and frozen at −20 °C (heparinized plasma) or −70 °C (EDTA plasma) until analysis. MMP-9 analysis was performed using a commercially available ELISA (R&D systems), according to the manufacturer's instruction. The mean coefficient of variation was 2.2 %. Samples were also diluted tenfold in phosphate-buffered saline (PBS) with non-reducing Laemmli sample buffer and then run on 4–20 % gradient SDS-PAGE gels containing 0.1 % gelatin. Gels were washed for 1 h in 2.5 % Triton X-100 and then incubated overnight at 37 °C in Novex developing buffer (Life Technologies, Grand Island, NY). Visualization of the gelatinolytic activity was performed with coomassie blue staining and destaining according to the manufacturer's instructions (Life Technologies, Grand Island, NY). Gel band density quantification was performed using ImageJ software (version 1.45, NIH, Bethesda, MD).

Statistical Analysis

Descriptive statistics of baseline variables and outcomes was performed, and reported as mean ± SD (for normally distributed continuous data), median with interquartile range (IQR; for non-normal or ordinal data) and proportions for binary data. Inter-rater agreement was assessed for stroke volume using intraclass correlation coefficient and Bland–Altman analyses [22].

For comparing results between the control and GAMES-Pilot subjects, Student t testing, Wilcoxon rank-sum testing, or Fisher exact tests were used as appropriate, depending on data type. For the repeated measures analysis of FLAIR ratio over time, repeated measures MANOVA was used. Statistical significance was taken at a two-sided p value of <0.05. Statistical analyses were performed using STATA 12 (College Station, TX) and JMP Pro 10.0 (Cary, NC).

Results

We used a retrospective, case–control design to evaluate the effect of IV glyburide on markers of edema compared to two matched control cohorts that were not treated with IV glyburide. The clinical characteristics of the GAMES-Pilot subjects and the matched control cohorts are shown in Table 1. The GAMES-Pilot subjects were acute stroke patients with large hemispheric stroke treated with IV glyburide within 10 h of stroke onset who had MRIs at baseline and days 1, 2, and 3 after stroke. The neuroimaging control

Table 1 Clinical characteristics of the cohorts

	GAMES-Pilot ($N = 10$)	Neuroimaging controls ($N = 8$)	Two-sided p value[a]	Biomarker controls ($N = 15$)	Two-sided p value[b]
Age, mean ± SD	51 ± 15	63 ± 12	0.07	74 ± 14	**<0.01**
Male % (n)	30 % (3)	88 % (7)	**0.02**	60 % (9)	0.23
Baseline NIHSS, median (IQR)	19 [15, 23]	19 [16, 21]	0.72	17 [15, 23]	0.68
Baseline DWI volume (cm^3), mean ± SD	102 ± 23	117 ± 68	0.55	117 ± 38	0.22
Admission glucose (mg/dL), mean ± SD	123 ± 16	138 ± 28	0.33	129 ± 21	0.43
Medical history % (n)					
Hypertension	50 % (5)	63 % (5)	0.66	67 % (10)	0.44
Diabetes	20 % (2)	13 % (1)	1.00	0 % (0)	0.15
Hyperlipidemia	30 % (3)	63 % (5)	0.34	40 % (6)	0.69
Prior ischemic stroke	40 % (4)	0 % (0)	0.09	27 % (4)	0.67
Atrial fibrillation	10 % (1)	25 % (2)	0.56	60 % (9)	**0.02**
Coronary artery disease	10 % (1)	25 % (2)	0.56	13 % (2)	1.00
Intravenous thrombolysis % (n)	90 % (9)	0 % (0)	**<0.01**	80 % (12)	1.00

Bold values are statistically significant ($p < 0.05$)

[a] Comparison between GAMES-Pilot and neuroimaging cohort

[b] Comparison between GAMES-Pilot and biomarker cohort

cohort was derived from placebo-treated subjects in the NBO. Eight placebo-treated subjects with large hemispheric stroke had similarly timed serial brain MRIs at baseline and at days 1 and 2 after stroke onset. Compared to neuroimaging controls, GAMES-Pilot subjects were more commonly female and more frequently treated with IV tissue plasminogen activator (tPA). The biomarker control cohort was the subset of large hemispheric stroke subjects ($N = 12$) from the specialized program of translational research in acute stroke (SPOTRI-AS) biomarker study [23], which had available blood samples drawn at approximately 48 h after stroke onset. Compared to the biomarker controls, GAMES-Pilot subjects were younger in age and had a lower frequency of atrial fibrillation (Table 1).

Cytotoxic Edema

Given prior work demonstrating an effect of glyburide on cytotoxic edema in cell models [20], we assessed whether IV glyburide influenced a brain MRI marker of cytotoxic edema in human patients. The ADC map is sensitive to cytotoxic edema within minutes after stroke [9], with the initial cytotoxic injury reaching its greatest extent after approximately 24 h [24, 25]. Figure 1a shows examples of ADC maps at baseline (<9 h after stroke onset) and after approximately 1 day in a control and a GAMES subject. There was no difference in ADC values at the baseline scan, which was obtained prior to initiation of the IV glyburide infusion. A reduction in relative ADC intensity was visible within the stroke region between the baseline and day-1 MRI, a pattern which is consistent with prior reports [24]. However, there were no differences between ADC values at day 1 when comparing the control and glyburide-treated subjects. Quantitative analysis of the relative ADC ratio (Fig. 1b) confirmed that ADC values were not influenced by IV glyburide.

Vasogenic Edema and T2 FLAIR Signal Intensity

Glyburide has been reported to reduce vasogenic edema and preserve the integrity of the BBB in animal models [21]. Leveraging the sensitivity of T2 FLAIR MRI to vasogenic edema [13], we evaluated the FLAIR signal intensity ratios in GAMES-Pilot compared to NBO comparison cohort. Figure 2a shows an example of a diffusion-weighted image (DWI) delineating the stroke volume and the corresponding FLAIR lesion in a control subject (top panels) and in a patient treated with IV glyburide (bottom panels). Quantitative assessment of the FLAIR ratio in the NBO cohort showed a rapid rise in values that plateaued after approximately 36 h from the onset of stroke (Fig. 2b). In contrast, the IV glyburide-treated group showed a blunted rise in the FLAIR ratio compared to control that began to diverge at approximately 24 h after stroke onset and persisted thereafter ($p < 0.005$). Although there were no available day-3 MRI scans in the control cohort for comparison, the FLAIR ratio did not rise further in the GAMES-Pilot cohort at that time point, suggesting persistence of the effect.

Following segmentation of the lesions into GM and WM, the FLAIR ratio values were reduced in both regions

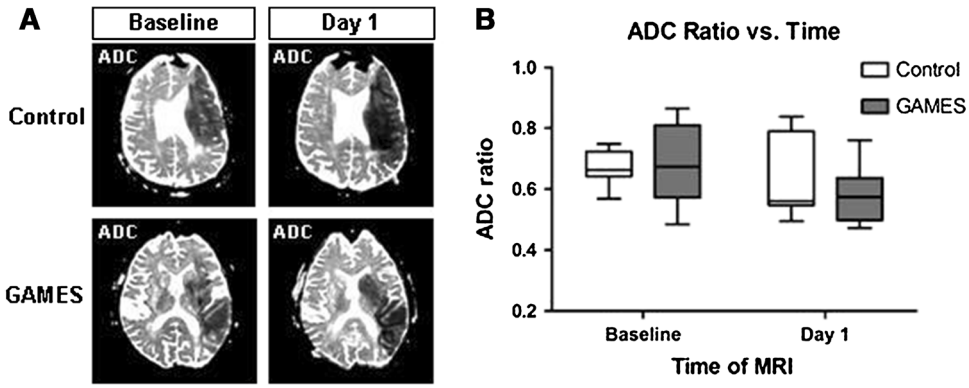

Fig. 1 Cytotoxic edema is not altered by glyburide treatment in human stroke. **a** Representative examples of apparent diffusion coefficient (ADC) maps in a control subject (*top panels*) and a glyburide-treated subject (*bottom panels*). The initial baseline ADC maps were obtained at approximately 7 h after onset of the stroke symptoms (*lefthand panels*), and the follow-up ADC maps were obtained at about 32 h after stroke onset. **b** Quantitative analysis of the control and glyburide (GAMES) cohorts show a similar decrease in relative ADC values from the baseline to day-1 MRI scan, but no difference between the two groups at either time point. *Box plots* show the median and interquartile range, and *whiskers* show the range

in the presence of IV glyburide (Fig. 2c). Given the effect of IV glyburide on FLAIR ratio, we reasoned that circulating glyburide concentration would correlate with the degree of FLAIR hyperintensity. We evaluated the association between FLAIR ratio and glyburide concentration in the GAMES-Pilot subjects at days 2 and 3, and found a concentration-dependent effect on FLAIR ratio (Spearman $r = -0.92$, $p < 0.001$). Next, we divided GAMES-Pilot subjects into low and high glyburide groups, dichotomized at the median concentration of 23 ng/mL. This threshold also corresponded to the plasma glyburide concentration in the phase-I safety study that resulted in subtly decreased blood glucose levels relative to baseline ($\sim$25 ng/mL; S. Jacobson, personnel communication). Using this as a pharmacodynamic surrogate, the average plasma glyburide concentration in the low-level group was 16 ± 4 and 31 ± 6 ng/mL in the high-level group. Figure 2d demonstrates a dose-dependent relationship between the FLAIR ratio and glyburide level in these subjects ($p = 0.014$).

Vasogenic Edema and Water Diffusion

To further test the hypothesis that IV glyburide attenuates vasogenic edema, we evaluated ADC values which begin to increase the first day after stroke due to increased water movement from the intravascular space into the brain [24, 26–28]. This net inflow increases the diffusivity of water within the brain, resulting in increased ADC values, a phenomenon termed pseudo-normalization [29]. The rate of pseudo-normalization is hypothesized to reflect the development of vasogenic edema [14, 24]. We, therefore, evaluated the change in ADC value from day 1 to day 2 in control and GAMES-Pilot subjects. The top panels in Fig. 3a show ADC maps from a control patient compared to a GAMES-Pilot patient (bottom panels). An increase in pseudo-normalization is evident in the control and noted by the change in ADC values from day 1 to day 2 (Fig. 3b). In contrast, the ADC ratio in GAMES-Pilot subjects remained essentially stable throughout this critical period for edema development.

In order to exclude the possibility that baseline imbalances between the two neuroimaging cohorts could account for the effect on FLAIR ratio and ADC pseudo-normalization, we assessed whether those variables were associated with the imaging measures. Importantly, sex did not demonstrate an association with the imaging metrics of vasogenic edema (FLAIR ratio $p = 0.43$ and ADC pseudo-normalization $p = 0.73$, both Wilcoxon rank-sum testing). The second difference between the GAMES-Pilot and neuroimaging control cohort was the rate of IV tPA treatment. Prior work has demonstrated that IV tPA increases the rate of pseudo-normalization [14], which should increase the rate of ADC pseudo-normalization in the GAMES-Pilot subjects, not reduce it. This would, therefore, be expected to bias results toward the null. Thus, neither of these factors is likely to account for the observed differences in imaging measures.

Vasogenic Edema and MMP-9

We next sought to further support the notion that IV glyburide attenuates vasogenic edema. MMP-9 is a zinc-dependent protease that is upregulated following cerebral infarction in both experimental models of stroke [15, 30] and in patients [31]. Excessive elevation in MMP-9 is associated with disturbed BBB integrity, vasogenic edema, and

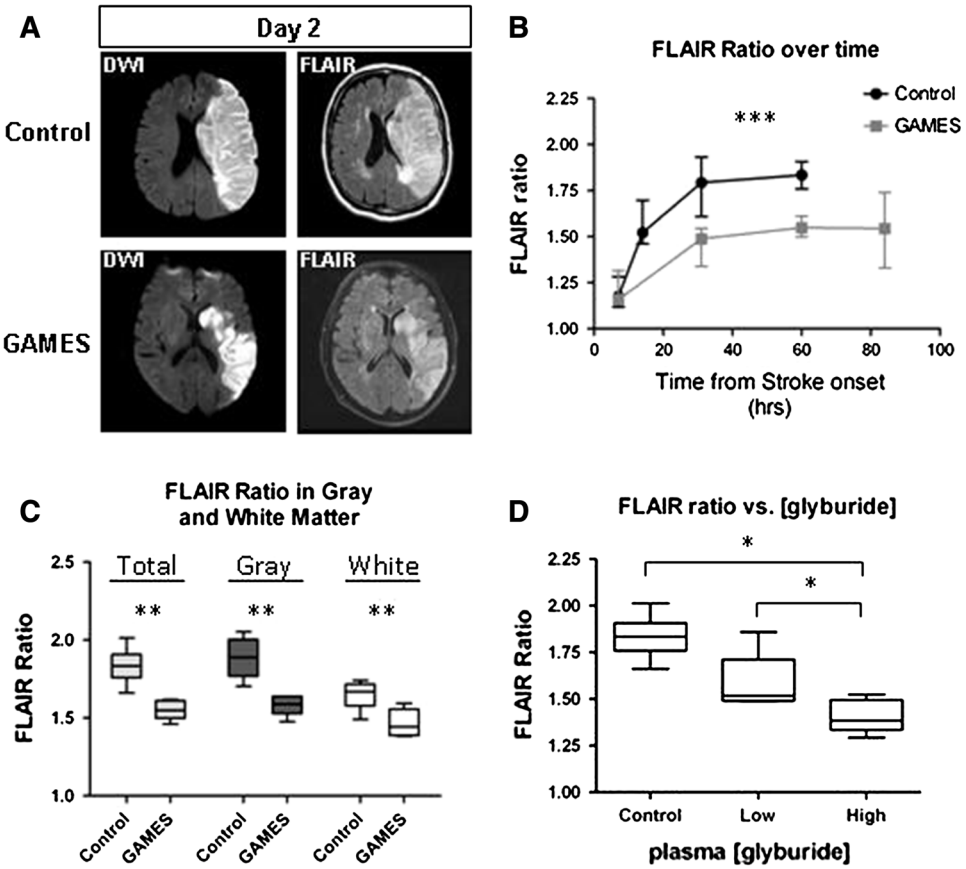

Fig. 2 Vasogenic edema on T2 FLAIR is attenuated by glyburide treatment in human stroke. **a** Representative examples of DWI (*lefthand panels*) and FLAIR sequences (*righthand panels*) from a control subject (*top panels*) and a glyburide-treated subject (*bottom panels*). MRI scans were obtained at day 2 from the onset of stroke. **b** Quantitative analysis of the FLAIR ratio in control and GAMES subjects shows a reduced FLAIR ratio with glyburide treatment. *Dots* represent median, *whiskers* are the interquartile range. ***$p < 0.005$ by repeated measures MANOVA. **c** Segmentation of the stroke lesions demonstrate an equivalent effect of glyburide on both gray and white matter regions. *Box plots* show the median and interquartile range, and *whiskers* show the range. **$p < 0.01$. **d** The pharmacokinetic concentration of glyburide correlates with FLAIR ratio intensity in the GAMES-Pilot subjects. Glyburide concentration was dichotomized at 25 ng/mL (see text). The FLAIR ratio values were higher at the low glyburide concentration group compared to the high concentration group. *Box plots* show the median and interquartile range, and *whiskers* show the range. *$p = 0.01$

increased risk of hemorrhagic transformation [17, 32, 33]. Using a quantitative sandwich ELISA, we assessed MMP-9 in the GAMES-Pilot subjects samples over time (Fig. 4a). We next compared the level of MMP-9 to a control cohort with similarly large infarction at approximately 48 h after stroke onset (Fig. 4b). At this time point, subjects treated with IV glyburide had a mean MMP-9 level of 54 ± 17 ng/mL compared to 212 ± 151 ng/mL in the comparison cohort ($p < 0.01$). The control values we obtained are similarly elevated compared to the previously reported MMP-9 in patients with large hemispheric infarction [34].

Figure 4c shows zymographic analysis of MMP-9 activity in several representative control and GAMES-Pilot plasma samples. Quantification of the MMP-9 bands in all samples confirmed that total MMP-9 activity was reduced in a manner consistent with the ELISA results (Fig. 4d). Furthermore, gel zymography showed that IV glyburide attenuated the pro-enzyme but not the active form of MMP-9 (Fig. 4d; 0.78 ± 0.36 in GAMES-Pilot vs. 3.46 ± 2.58 in control, $p = 0.004$). Finally, MMP-9 circulates in the blood in association with tissue inhibitor of metalloproteinase 1 (TIMP-1) [35, 36], which may regulate the activity level of MMP-9. However, we found no difference in TIMP-1 level in the presence or absence of IV glyburide (161 ± 142 ng/mL in GAMES-Pilot vs. 154 ± 82 ng/mL in controls, $p = 0.90$). Taken together, these data suggest that GAMES-Pilot subjects had lower MMP-9 but similar levels of TIMP-1 level.

Discussion

Our data provide three concordant lines of evidence that IV glyburide is associated with alteration of vasogenic edema

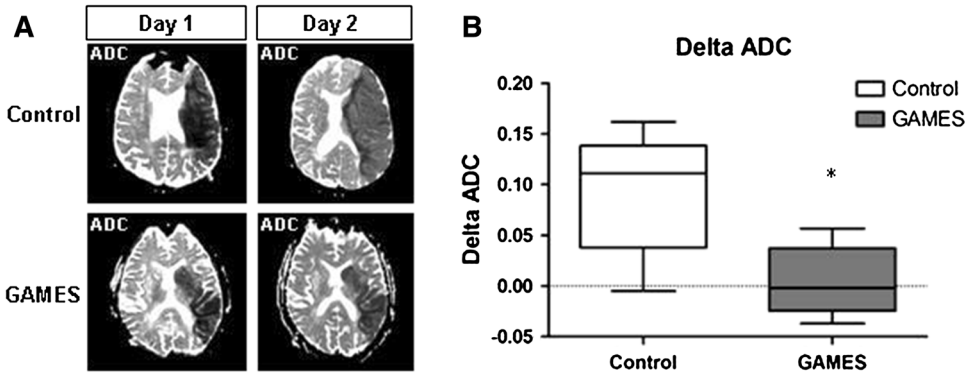

Fig. 3 Vasogenic edema measured by ADC pseudonormalization is attenuated by glyburide treatment in human stroke. **a** Representative example of ADC maps showing an increase in value between day 1 and day 2, which corresponds to increasing water diffusivity from edema formation. The *top panels* show a control subject and the *bottom panels* show a subject treated with IV glyburide. **b** Water diffusivity is increased in control subjects compared to GAMES subjects between days 1 and 2. There is less change in the ADC values within the stroke lesion in GAMES subjects ($*p = 0.028$). *Box plots* show the median and interquartile range, and *whiskers* show the range

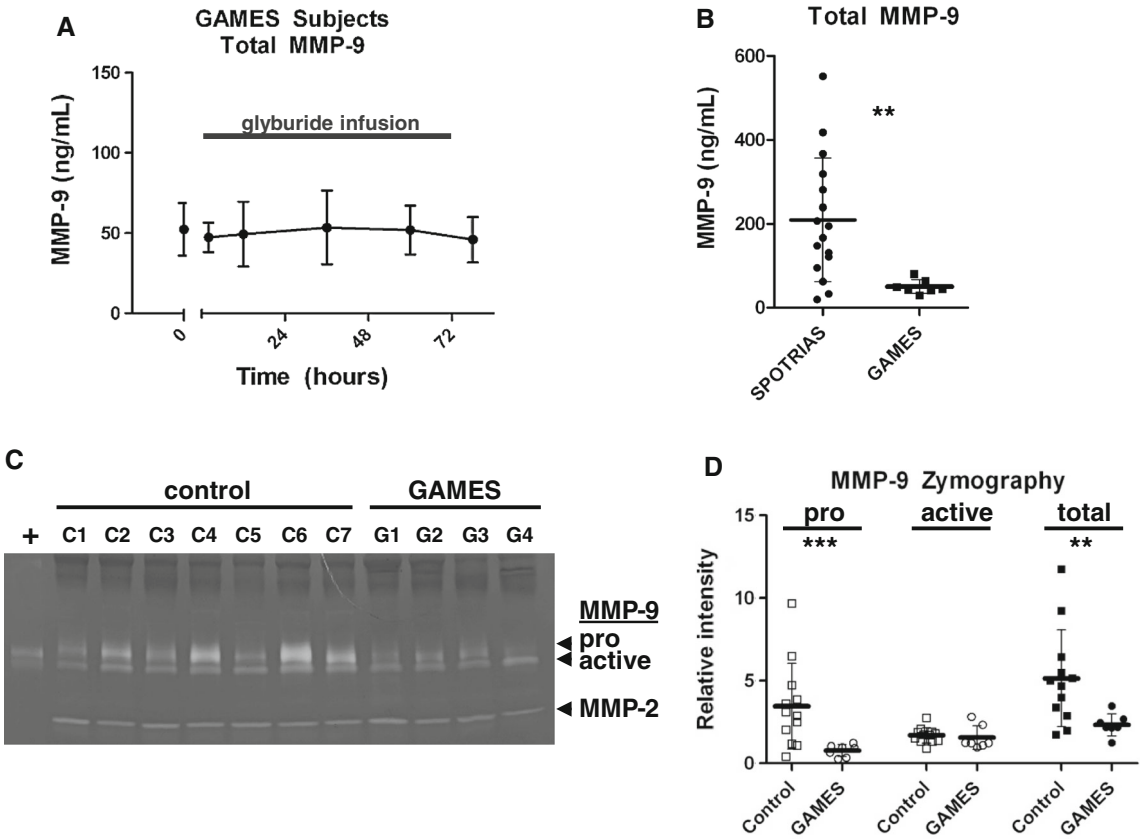

Fig. 4 MMP-9 level is reduced by glyburide treatment in human stroke. **a** Time course of total MMP-9 level in the GAMES subjects, measured by ELISA. The baseline MMP-9 prior to infusion is shown at time 0, and the timing of IV glyburide is indicated by the *bar*. **b** Total MMP-9 at approximately 36 h after stroke onset in the SPOTRIAS control and GAMES cohorts. *Bars* represent the mean, *whiskers* represent the SD. $**p < 0.01$. **c** Representative gelatin zymography analysis of MMP-9 in the control and GAMES cohorts. The pro-enzyme migrates slightly higher that the active form of MMP-9. MMP-2 is also detectable using this method. **d** Band intensity quantitation of gelatin zymography shows that glyburide reduces the level of the pro-MMP-9 enzyme but not the active form ($p = 0.68$). *Bars* represent the mean, *whiskers* represent the SD. $***p < 0.005$, $**p < 0.01$

after ischemic stroke. The glyburide-associated attenuation of the MRI FLAIR ratio, the ADC pseudo-normalization rate, and the reduction in circulating MMP-9 together raise the possibility that markers of vasogenic edema may be modifiable in human stroke patients. These findings are consistent with preclinical evidence that glyburide reduces brain edema [19]. Although our current data do not support an association between IV glyburide and cytotoxic edema, this apparent discrepancy may be due to several reasons. The timing at which glyburide is started relative to onset of ischemia may be important. In this regard, glyburide was effective in cell models when present at the onset of ischemia [20], whereas IV glyburide treatment in GAMES-Pilot patients was started at about 9 h after stroke onset. Alternatively, our analysis may not be powered to detect small differences in cytotoxic edema measured by ADC ratio. Future studies in the later phase clinical development of IV glyburide may help shed further light on this discrepancy.

Our data also highlight novel directions for the clinical development of IV glyburide. The reduction in MMP-9 raises the additional possibility that IV glyburide may attenuate BBB injury and hemorrhagic transformation. Elevated MMP-9 is associated with increased risk of hemorrhage after stroke [17], particularly in the setting of IV tPA [32]. In this context, inhibition of MMP-9 reduces hemorrhage in preclinical stroke models [37] and glyburide is reported to reduce MMP-9 in cell culture [21]. Our finding that IV glyburide is associated with lower MMP-9 in human patients suggests that it may be worthwhile to test its ability to reduce hemorrhagic transformation in future studies. This concept is supported by a recent retrospective analysis showing an association between sulfonylurea usage and reduced risk of hemorrhagic transformation in diabetics with acute ischemic stroke [38]. Given that hemorrhagic transformation rates range from 15 to 30 % [39, 40], definitive analysis would require a larger, placebo-controlled study. In the interim, the rate of hemorrhagic transformation would be an important secondary outcome in subsequent phase II or phase III evaluation of IV glyburide in edema prevention.

Our study has several important limitations. Despite several lines of evidence that support an effect on vasogenic edema, it is important to acknowledge that these are intermediate markers which have not been validated as surrogates for clinical outcome. In this context, our intermediate surrogate data on vasogenic edema represent a critical but insufficient step in the process of demonstrating clinical efficacy of this compound. Our analysis is also restricted to a small number of patients with some baseline imbalances in the cohorts. Since alternative cohorts with similarly timed daily research MRIs and blood samples were not available, this represented the best available case–controls for comparison. Furthermore, none of the baseline imbalances were associated with the measures of vasogenic edema or, in the case of IV tPA, would bias against the detection of an effect. Finally, our analysis is restricted to the subpopulation of large hemispheric infarction, and is not generalizable to all strokes. Future studies looking at the spectrum of infarct sizes are warranted to assess the utility of these metrics on a broader scale.

Summary

To date, there are few options in the management of ischemic cerebral edema. The prospect of preventing secondary neurological injury represents a novel strategy in acute stroke therapy. Our data demonstrate that IV glyburide is associated with several markers of vasogenic edema in stroke patients. Future studies that validate the generalizability of these markers, combined with the next phase clinical development will provide insight into whether targeting ischemic cerebral edema with IV glyburide has further merit.

Acknowledgments This work was supported by the National Institutes of Health/National Institute of Neurological Diseases and Stroke (K23 NS076597, W.T.K.). Some of the samples and data used in this research were originally collected with funding through the NIH (P50 NS051343, K.L.F. and R01 NS051412, A.B.S.) or through Remedy Pharmaceuticals, Inc (GAMES-Pilot study).

Disclosures W.T.K discloses a research Grant (NIH; significant). The GAMES-Pilot study (NCT01268683) was funded by Remedy Pharmaceuticals, Inc. and the sponsor had no role in the preparation of this manuscript.

References

1. Simard JM, Kent TA, Chen M, Tarasov KV, Gerzanich V. Brain oedema in focal ischaemia: molecular pathophysiology and theoretical implications. Lancet Neurol. 2007;6:258–68.
2. Ayata C, Ropper AH. Ischaemic brain oedema. J Clin Neurosci. 2002;9:113–24.
3. Kimberly WT, Sheth KN. Approach to severe hemispheric stroke. Neurology. 2011;76:S50–6.
4. Hacke W, Schwab S, Horn M, Spranger M, De Georgia M, von Kummer R. 'Malignant' middle cerebral artery territory infarction: clinical course and prognostic signs. Arch Neurol. 1996;53:309–15.
5. Vahedi K, Hofmeijer J, Juettler E, et al. Early decompressive surgery in malignant infarction of the middle cerebral artery: a pooled analysis of three randomised controlled trials. Lancet Neurol. 2007;6:215–22.
6. Hofmeijer J, Kappelle LJ, Algra A, et al. Surgical decompression for space-occupying cerebral infarction (the hemicraniectomy after middle cerebral artery infarction with life-threatening edema trial [HAMLET]): a multicentre, open, randomised trial. Lancet Neurol. 2009;8:326–33.

7. van der Worp HB, Kappelle LJ. Early decompressive hemicraniectomy in older patients with nondominant hemispheric infarction does not improve outcome. Stroke. 2011;42:845–6.
8. Klatzo I. Presidental address. Neuropathological aspects of brain edema. J Neuropathol Exp Neurol. 1967;26:1–14.
9. Neumann-Haefelin T, Moseley ME, Albers GW. New magnetic resonance imaging methods for cerebrovascular disease: emerging clinical applications. Ann Neurol. 2000;47:559–70.
10. Todd NV, Picozzi P, Crockard A, Russell RW. Duration of ischemia influences the development and resolution of ischemic brain edema. Stroke. 1986;17:466–71.
11. Bell BA, Symon L, Branston NM. CBF and time thresholds for the formation of ischemic cerebral edema, and effect of reperfusion in baboons. J Neurosurg. 1985;62:31–41.
12. Crockard A, Iannotti F, Hunstock AT, Smith RD, Harris RJ, Symon L. Cerebral blood flow and edema following carotid occlusion in the gerbil. Stroke. 1980;11:494–8.
13. Schaefer PW. Diffusion-weighted imaging as a problem-solving tool in the evaluation of patients with acute strokelike syndromes. Top Magn Reson Imaging. 2000;11:300–9.
14. Marks MP, Tong DC, Beaulieu C, Albers GW, de Crespigny A, Moseley ME. Evaluation of early reperfusion and i.v. tPA therapy using diffusion- and perfusion-weighted MRI. Neurology. 1999; 52:1792–8.
15. Rosenberg GA, Estrada EY, Dencoff JE. Matrix metalloproteinases and TIMPs are associated with blood-brain barrier opening after reperfusion in rat brain. Stroke. 1998;29:2189–95.
16. Zhao BQ, Tejima E, Lo EH. Neurovascular proteases in brain injury, hemorrhage and remodeling after stroke. Stroke. 2007; 38:748–52.
17. Castellanos M, Leira R, Serena J, et al. Plasma metalloproteinase-9 concentration predicts hemorrhagic transformation in acute ischemic stroke. Stroke. 2003;34:40–6.
18. Chen M, Simard JM. Cell swelling and a nonselective cation channel regulated by internal Ca^{2+} and ATP in native reactive astrocytes from adult rat brain. J Neurosci. 2001;21:6512–21.
19. Simard JM, Chen M, Tarasov KV, et al. Newly expressed SUR1-regulated NC(Ca-ATP) channel mediates cerebral edema after ischemic stroke. Nat Med. 2006;12:433–40.
20. Chen M, Dong Y, Simard JM. Functional coupling between sulfonylurea receptor type 1 and a nonselective cation channel in reactive astrocytes from adult rat brain. J Neurosci. 2003; 23:8568–77.
21. Simard JM, Geng Z, Silver FL, et al. Does inhibiting Sur1 complement rt-PA in cerebral ischemia? Ann N Y Acad Sci. 2012;1268:95–107.
22. Bland JM, Altman DG. Statistical methods for assessing agreement between two methods of clinical measurement. Lancet. 1986;1:307–10.
23. Kimberly WT, Wang Y, Pham L, Furie KL, Gerszten RE. Metabolite profiling identifies a branched chain amino acid signature in acute cardioembolic stroke. Stroke. 2013;44(5):1389–95.
24. Schwamm LH, Koroshetz WJ, Sorensen AG, et al. Time course of lesion development in patients with acute stroke: serial diffusion- and hemodynamic-weighted magnetic resonance imaging. Stroke. 1998;29:2268–76.
25. Warach S, Chien D, Li W, Ronthal M, Edelman RR. Fast magnetic resonance diffusion-weighted imaging of acute human stroke. Neurology. 1992;42:1717–23.
26. Chien D, Kwong KK, Gress DR, Buonanno FS, Buxton RB, Rosen BR. MR diffusion imaging of cerebral infarction in humans. AJNR Am J Neuroradiol. 1992;13:1097–102; discussion 103–5.
27. Welch KM, Windham J, Knight RA, et al. A model to predict the histopathology of human stroke using diffusion and T2-weighted magnetic resonance imaging. Stroke. 1995;26:1983–9.
28. Schlaug G, Siewert B, Benfield A, Edelman RR, Warach S. Time course of the apparent diffusion coefficient (ADC) abnormality in human stroke. Neurology. 1997;49:113–9.
29. Warach S, Gaa J, Siewert B, Wielopolski P, Edelman RR. Acute human stroke studied by whole brain echo planar diffusion-weighted magnetic resonance imaging. Ann Neurol. 1995;37: 231–41.
30. Romanic AM, White RF, Arleth AJ, Ohlstein EH, Barone FC. Matrix metalloproteinase expression increases after cerebral focal ischemia in rats: inhibition of matrix metalloproteinase-9 reduces infarct size. Stroke. 1998;29:1020–30.
31. Montaner J, Alvarez-Sabin J, Molina C, et al. Matrix metalloproteinase expression after human cardioembolic stroke: temporal profile and relation to neurological impairment. Stroke. 2001;32:1759–66.
32. Montaner J, Molina CA, Monasterio J, et al. Matrix metalloproteinase-9 pretreatment level predicts intracranial hemorrhagic complications after thrombolysis in human stroke. Circulation. 2003;107:598–603.
33. Castellanos M, Sobrino T, Millan M, et al. Serum cellular fibronectin and matrix metalloproteinase-9 as screening biomarkers for the prediction of parenchymal hematoma after thrombolytic therapy in acute ischemic stroke: a multicenter confirmatory study. Stroke. 2007;38:1855–9.
34. Serena J, Blanco M, Castellanos M, et al. The prediction of malignant cerebral infarction by molecular brain barrier disruption markers. Stroke. 2005;36:1921–6.
35. Chakraborti S, Mandal M, Das S, Mandal A, Chakraborti T. Regulation of matrix metalloproteinases: an overview. Mol Cell Biochem. 2003;253:269–85.
36. Yong VW, Power C, Forsyth P, Edwards DR. Metalloproteinases in biology and pathology of the nervous system. Nat Rev Neurosci. 2001;2:502–11.
37. Wang X, Lee SR, Arai K, et al. Lipoprotein receptor-mediated induction of matrix metalloproteinase by tissue plasminogen activator. Nat Med. 2003;9:1313–7.
38. Kunte H, Busch MA, Trostdorf K, et al. Hemorrhagic transformation of ischemic stroke in diabetics on sulfonylureas. Ann Neurol. 2012;72:799–806.
39. Mlynash M, Lansberg MG, De Silva DA, et al. Refining the definition of the malignant profile: insights from the DEFUSE-EPITHET pooled data set. Stroke. 2011;42:1270–5.
40. Katzan IL, Furlan AJ, Lloyd LE, et al. Use of tissue-type plasminogen activator for acute ischemic stroke: the Cleveland area experience. JAMA. 2000;283:1151–8.